

Increasing entanglement between Gaussian states by coherent photon subtraction

Alexei Ourjoumtsev, Aurélien Dantan, Rosa Tualle-Brouri, and Philippe Grangier
 Laboratoire Charles Fabry de l'Institut d'Optique, CNRS UMR 8501, 91403 Orsay, France*
 (Dated: February 9, 2020)

We experimentally demonstrate that the entanglement between Gaussian entangled states can be increased by non-Gaussian operations. Coherent subtraction of single photons from Gaussian quadrature-entangled light pulses, created by a non-degenerate parametric amplifier, produces delocalized "Schrödinger kitten" states with complex negative Wigner functions, more entangled than the initial states in terms of negativity. The experimental results are in very good agreement with the theoretical predictions.

PACS numbers: : 03.67.-a, 03.65.Wj, 42.50.Dv

Entanglement distillation [1] plays a key role in quantum information processing (QIP). It allows to produce strong entanglement between distant sites, initially sharing a larger set of weakly entangled states, and constitutes the basis of quantum repeaters, essential for long-distance quantum communications. Entanglement distillation for discrete-variable systems (ebits) has been demonstrated in recent experiments [2, 3, 4]. An interesting alternative to discrete-level systems are quantum continuous variables (QCV). In this case the information is encoded in the quadratures \hat{x} and \hat{p} of travelling light fields, which can be efficiently measured by homodyne detection. Optical parametric amplification allows to produce quadrature-entangled beams, used in many QIP protocols. Together with linear optics, these tools preserve the Gaussian character of the states involved in most of QCV experiments: the quasi-distributions (Wigner functions) of their quadratures remain Gaussian. However, it has been shown that Gaussian entanglement distillation requires non-Gaussian operations [5, 6, 7]. Among several proposals [8, 9], one of the simplest is the conditional subtraction of photons from Gaussian entangled beams [10, 11, 12, 13], by reflecting a small part of these beams towards two avalanche photodiodes (APDs) operating in a photon-counting regime. If the reflectivity is sufficiently low, a simultaneous detection of photons by the APDs heralds the subtraction of exactly one photon from each beam. Recently, such methods have allowed to prepare and analyze several states with negative Wigner functions, including one and two photon Fock states [14, 15, 16], delocalized single photons [17, 18] and "Schrödinger kitten" states [19, 20]

In this Letter, we demonstrate the possibility to distill entanglement from Gaussian states with a modified version of the protocol above, presented on Fig. 1. An optical parametric amplifier (OPA) produces Gaussian quadrature-entangled light pulses, usually known as two-mode squeezed states [21]. We pick off small fractions of these beams, which interfere with a well-defined phase on a 50/50 beamsplitter (BS), and we detect photons in one of the BS outputs. This way, we subtract a *single* photon delocalized in the two beams and prepare a complex quantum state with a negative two-mode Wigner function, which can be considered as a delocalized "Schrödinger kitten" state [19], revealed by measuring the correlations between the entangled beams. We determine a range of experimental parameters where the entanglement of

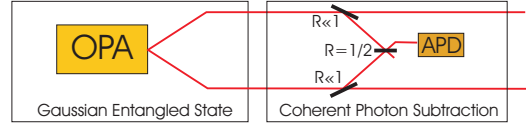


FIG. 1: Entanglement distillation from Gaussian states

the prepared state, quantified by the negativity [22], is significantly higher compared to that of the initial Gaussian state.

This protocol, operating with single photon counts rather than with coincidences as proposed e. g. in [10, 11, 12, 13, 23, 24], works with much higher generation rates and produces states more robust to experimental imperfections (see below). Besides, it is more efficient at moderate OPA gain: in the zero-gain limit, the detection of a photon transforms a state with almost no entanglement into a maximally entangled ebit state $(|10\rangle + |01\rangle)/\sqrt{2}$. With the higher gain (up to 3 dB) used in the present experiment, the generated states have a much richer structure as it will be shown below.

Our experimental setup is presented on Fig. 2. Nearly Fourier-limited femtosecond pulses (180 fs, 40 nJ), produced by a Ti-Sapphire laser with a 800 kHz repetition rate, are frequency-doubled by a single pass in a 100 μm -thick type I non-critically phase-matched potassium niobate (KNbO₃) crystal. The frequency-doubled beam pumps an identical

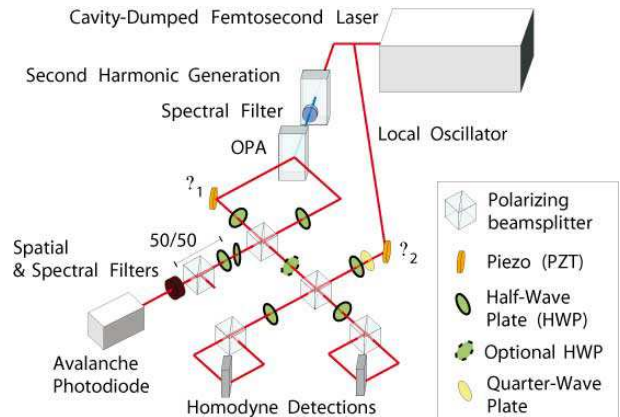


FIG. 2: Experimental setup

crystal used as an optical parametric amplifier (OPA), generating Gaussian quadrature-entangled pulses spatially separated by an angle of 10° . Adjusting the pump power allows to vary the two-mode squeezing between 0 and 3.5 dB. The photon pick-off beam splitters are realized with a single polarizing beam splitter cube (PBS), where the signal and idler beams are recombined spatially but remain separated in polarization. A small adjustable fraction R of both beams is sent into the APD channel, where they interfere on a 50/50 BS. A tilted half-wave plate compensates for residual birefringence. An APD detects one of the 50/50 BS outputs after spatial and spectral filtering. The signal and idler beams transmitted through the pick-off beamsplitter are projected into a non-Gaussian state by an APD detection. They are spatially separated on another PBS, where they are combined with bright local oscillator beams. A quarter-wave and a half-wave plate allow to prepare two local oscillators with equal intensities and a well-defined relative phase. The signal and idler beams are analyzed by two time-resolved homodyne detections, which sample each individual pulse, measuring one quadrature $x_{1,2}(\theta_{1,2})$ in phase with the local oscillator.

In this setup, all the phases except ϕ_1 and ϕ_2 (corresponding to the two PZT on Fig. 2) are precisely adjusted with wave plates. But a relative phase shift ϕ_1 between the signal and the idler beam only modifies the direction of the two-mode squeezed ellipse. A change in this direction can be compensated by shifting the common phase ϕ_2 of the local oscillators. This phase can be scanned with a PZT, and rapidly measured using the unconditioned two-mode squeezing variance between the homodyne detections.

Quantum states with negative Wigner functions are very fragile, and all the experimental imperfections must be minimized. In our case, the most important issue is that an APD detection does not always correspond to the desired photon subtraction, because of imperfect filtering, limited spectral and spatial qualities of the optical beams, imperfect mode-matching between the subtracted beams, and APD dark counts. An APD count corresponds to the right event with a success probability $\xi < 1$. This explains why single-photon protocols are more robust than two-photon ones, where the total success probability is only ξ^2 . Another issue is the OPA excess noise. To describe it, we can consider that a first amplification process creates a pure entangled state with a two-mode squeezing variance $s = e^{-2r}$, and that each of the resulting modes is independently amplified with a gain $h = \cosh^2(\gamma r)$ by a phase-independent amplifier with a relative efficiency γ . The finite homodyne efficiency η and the homodyne excess noise e also deteriorate the measured data. However, they are not involved in the generation process but only in the analysis, and we can correct for their effects in order to determine the actual Wigner function of the generated state. Even with none of these imperfections, this distillation protocol would still be limited by the finite pick-off BS reflectivity R , which is required to have a sufficient APD count rate but induces losses on the transmitted beam. The limited overall efficiency $\mu = 5\%$ of the APD channel, including the filtering system,

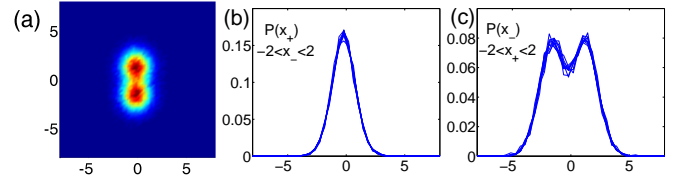


FIG. 3: State separability test after interference between signal and idler beams : (a) Joint distribution $P(x_+, x_-)$, (b) Distributions $P(x_+)$ for $-2 < x_- < 2$, (c) Distributions $P(x_-)$ for $-2 < x_+ < 2$. Here $\theta_+ = 20^\circ$ and $\theta_- = 50^\circ$, the same result holds for all θ_{\pm} .

has little effect in this experiment.

A detailed analytic model [16, 19], taking all the experimental imperfections into account, yields an expression for the Wigner function W of the state studied in our experiment :

$$W(x_1, p_1, x_2, p_2) = W_s \left(\frac{x_1 + x_2}{\sqrt{2}}, \frac{p_1 + p_2}{\sqrt{2}} \right) W_c \left(\frac{x_1 - x_2}{\sqrt{2}}, \frac{p_1 - p_2}{\sqrt{2}} \right) \quad (1)$$

where W_s is the Wigner function of a single-mode squeezed state, and W_c corresponds to a single-mode "Schrödinger kitten" state, analyzed in [19]. More explicitly :

$$W_s(x, p) = \frac{\exp(-x^2/a - p^2/b)}{\pi\sqrt{ab}}$$

$$W_c(x, p) = W_s(x, p) \left[\frac{2A}{a^2}x^2 + \frac{2B}{b^2}p^2 + 1 - \frac{A}{a} - \frac{B}{b} \right]$$

$$a(s) = b(1/s) = 1 + e + \eta(1 - R)(hs + h - 2)$$

$$A(s) = B(1/s) = \frac{\eta \xi (1 - R)(hs + h - 2)^2}{h(s + 1/s) + 2h - 4}$$

In this experiment the "Schrödinger kitten" state is "delocalized" into two spatially separated modes 1 and 2 and revealed by measuring the correlations between identical quadratures, the anticorrelations remaining in the initial squeezed state.

Without assuming any particular shape for W_s and W_c , we can experimentally show that the state becomes separable if we make a joint measurement, transforming $x_{1,2}$ into $x_{+,-} = (x_1 \pm x_2)/\sqrt{2}$ by rotating the polarizations by 45° with the optional HWP shown on Fig. 2. We then observe that the quadratures measured by one detection do not depend on the other (see Fig. 3). For every θ_{\pm} the joint distribution, and hence the Wigner function, becomes factorable : $P(x_+(\theta_+), x_-(\theta_-)) = P(x_+(\theta_+))P(x_-(\theta_-))$. It means that one can fix $\theta_- = \theta_+ = \theta$ and scan θ to perform a complete tomography of this state.

This property considerably simplifies the experimental analysis of the generated entangled state. For measuring entanglement, we do not recombine the entangled modes 1 and 2, but keep them spatially separated and perform homodyne measurements of $x_{1,2}(\theta)$. The correlations between $x_1(\theta)$ and $x_2(\theta)$ correspond then to $x_-(\theta)$, and their anticorrelations to $x_+(\theta)$. In practice, we set the relative phase between the local oscillators to zero, scan the common phase $\phi_2 = \theta$, mea-

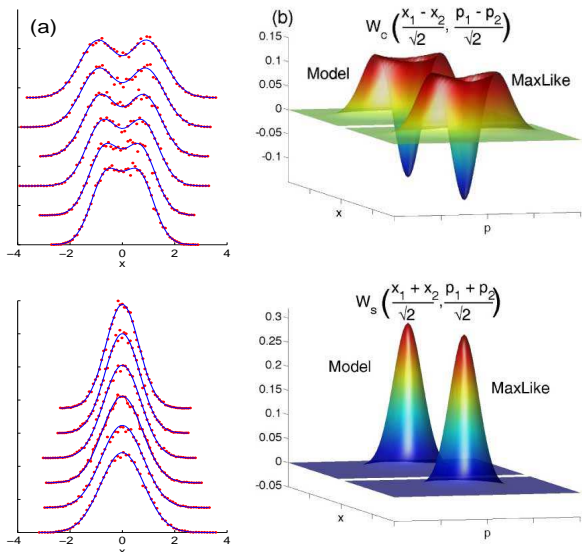


FIG. 4: (a) Set of experimentally measured quadrature distributions (dots), compared to those reconstructed from our model (solid line). (b) Wigner function corrected for homodyne detection losses, obtained with a standard Maximal-Likelihood algorithm (MaxLike), compared to the result of our model. This state is produced with 1.8 dB of squeezing and $R = 5\%$.

measure $x_{1,2}(\theta)$ and calculate $x_{+,-}(\theta)$. We reconstruct the distributions $P_c(x_-(\theta))$ and $P_s(x_+(\theta))$ for several phases. We observe that the measured distributions are invariant under $\theta \rightarrow \pi \pm \theta$, so we can restrict the analysis to $0 \leq \theta \leq \pi/2$. Typically, we measure 6 to 12 different quadrature distributions, with 10000 to 20000 data points each. A numeric Radon transform allows to reconstruct the uncorrected Wigner functions W_c and W_s . We can correct for the homodyne detection losses using a Maximal-Likelihood algorithm [25, 26] to obtain the Wigner function W and the density matrix ρ of the generated state, and calculate its entanglement, given by the negativity $\mathcal{N} = \frac{\|\rho^{T_1}\|_1 - 1}{2}$, where T_1 is the partial transposition operation [22].

Figure 4 presents the tomography of a state produced with 1.8 dB of squeezing and a BS reflectivity $R = 5\%$. The Wigner function, corrected for detection losses, is clearly negative: $W_c(0) = -0.13 \pm 0.01$. The entanglement of this state is $\mathcal{N} = 0.34 \pm 0.02$, whereas for the initial state (before the pick-off BS) $\mathcal{N}_0 = 0.24 \pm 0.01$.

In Refs. [16, 19] we demonstrated another analysis method, more constrained but also much faster and closer to the physics of the experiment. If we assume that the Wigner function has the form defined in Eq. 1, we can easily extract the parameters a, A, b, B from the second and fourth moments of the measured distributions, and determine the Wigner function, the density matrix and the quadrature distributions of the measured state. For a given squeezing, one can also obtain from a, A, b and B the values of all the experimental parameters introduced above. It allows to easily correct for homo-

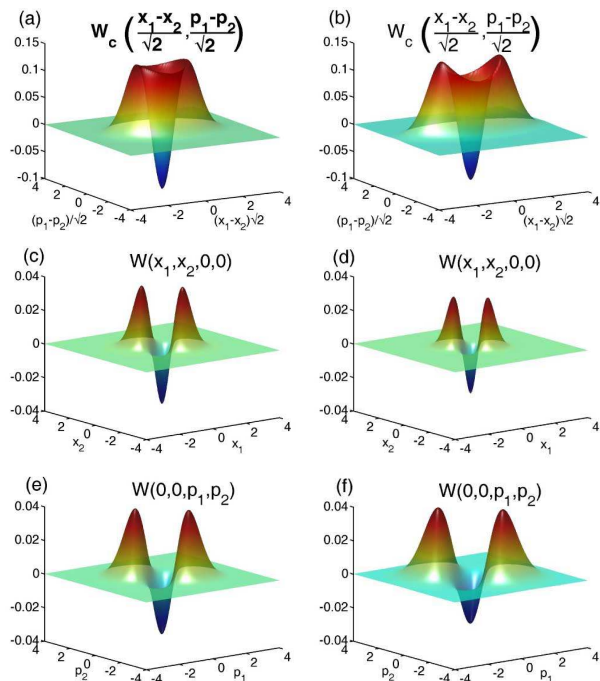


FIG. 5: Tomography of two states produced with 1.3 dB (left) and 3.2 dB (right) of squeezing and $R = 10\%$: three different projections of the two-mode Wigner function.

dyne losses: we simply calculate the Wigner function that we would measure with an ideal detection ($\eta = 1$ and $e = 0$), using the values extracted from the experimental data for all the other parameters. As shown in Fig. 4, the distributions reconstructed with this method are in excellent agreement with those directly extracted from the data, and the Wigner function corrected for losses is almost indistinguishable from the one obtained with the Maximal-Likelihood algorithm. Both methods give the same values for the negativity.

A natural question to ask is whether this protocol works for an arbitrary squeezing or if, when the initial state is already strongly entangled, by performing an imperfect photon subtraction we actually lose more entanglement than we gain. It has already been shown that, when the pick-off beam splitters have a finite reflectivity, subtracting one photon from each of the Gaussian entangled beams may actually decrease the entanglement [10]. Using our model, we can take into account all the other experimental parameters to derive an analytic expression for the partially-transposed density matrix, which can be diagonalized numerically in a few seconds to obtain the expected negativity of a given state. We found that the experimental imperfections have a very strong effect. For example, for an initial squeezing of 3 dB, the negativity increases ideally from $\mathcal{N}_0 = 0.50$ to $\mathcal{N} = 0.90$. If we assume $R = 3\%$ for the pick-off BS, then $\mathcal{N} = 0.81$, but if we include the average values of experimental parameters involved in the state preparation, $\langle \gamma \rangle = 0.22$ and $\langle \xi \rangle = 0.78$, \mathcal{N} drops down to 0.51, whereas for the initial state, only slightly affected by γ , $\mathcal{N}_0 = 0.49$.

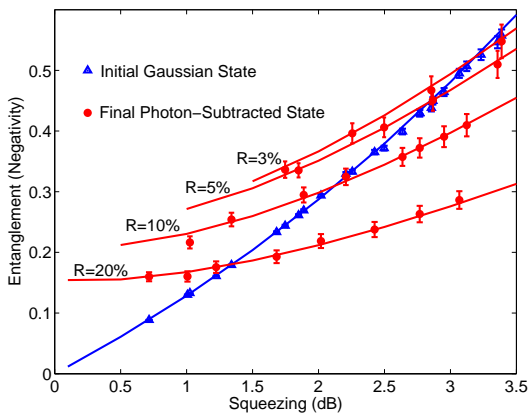


FIG. 6: Entanglement negativity of the initial and final states as a function of squeezing for several pick-off BS reflectivities, corrected for homodyne detection losses. Solid lines are theoretical calculations using the average values of the experimental parameters.

To verify this experimentally, we performed several tomographies for different BS reflectivities and degrees of squeezing. Figure 5 presents the results of two tomographies with $R = 10\%$ for a small (1.3 dB) and a high (3.2 dB) squeezing. As expected, the phase dependence of the generated state increases and the Wigner function becomes less negative, as the state becomes “bigger” and more sensitive to decoherence.

Figure 6 shows the entanglement negativity of the photon-subtracted states and of the corresponding initial states. Solid lines are theoretical calculations using the average values of the experimental parameters involved in the state preparation, $\langle \gamma \rangle = 0.22$ and $\langle \xi \rangle = 0.78$. Two domains appear on the graph: the upper left, where the photon subtraction actually increases the entanglement, and the lower right, where the initial state is too sensitive to the losses added by this process. As expected, this protocol is particularly advantageous at low squeezing. It is possible to show that when the squeezing, and hence the entanglement of the initial state, tend to 0, the negativity of the photon-subtracted state has a nonzero limit $\mathcal{N}_{r \rightarrow 0} = \frac{\sqrt{C^2 + (1-C)^2} - (1-C)}{2}$ where $C = \frac{\xi(1-R)}{1+\gamma^2}$. In the low squeezing regime, experimental imperfections have a moderate effect on the state. We nevertheless succeed in improving the negativity of a state with up to 3 dB of squeezing, which corresponds to a strong squeezing regime where small variations of the experimental parameters strongly affect the performance of the distillation protocol. For example, increasing ξ by a mere 4% with $R = 3\%$ should displace the crossover point from 3 to 4 dB (in other experiments, where mode-matching between subtracted photons was not an issue, we obtained $\xi = 0.9$ [16]).

As a conclusion, this purification protocol allows to increase the entanglement between Gaussian states with up to 3 dB of squeezing, and even small experimental improvements should significantly increase this limit. For QIP protocols specifically requiring Gaussian entanglement, these non-

Gaussian states could in principle be used as a starting point for a “Gaussification” procedure [9]. This demonstrates one of the key steps required for long distance quantum communications with continuous variables.

This work is supported by the EU IST/FET project COVAQIAL, and by the French ANR/PNANO project IRCOQ.

* Email : alexei.ourjountsev@institutoptique.fr

- [1] C. H. Bennett, H. J. Bernstein, S. Popescu, and B. Schumacher, *Phys. Rev. A* **53**, 2046 (1996).
- [2] P. G. Kwiat, S. Barraza-Lopez, A. Stefanov, and N. Gisin, *Nature* **409**, 1014 (2001).
- [3] J.-W. Pan, S. Gasparoni, R. Ursin, G. Weihs, and A. Zeilinger, *Nature* **423**, 417 (2003).
- [4] P. Walther, K. J. Resch, Č. Brukner, A. M. Steinberg, J.-W. Pan, and A. Zeilinger, *Phys. Rev. Lett.* **94**, 040504 (2005).
- [5] J. Eisert, S. Scheel, and M. B. Plenio, *Phys. Rev. Lett.* **89**, 137903 (2002).
- [6] J. Fiurášek, *Phys. Rev. Lett.* **89**, 137904 (2002).
- [7] G. Giedke and J. I. Cirac, *Phys. Rev. A* **66**, 032316 (2002).
- [8] L.-M. Duan, G. Giedke, J. I. Cirac, and P. Zoller, *Phys. Rev. Lett.* **84**, 4002 (2000).
- [9] J. Eisert, D. E. Browne, S. Scheel, and M. B. Plenio, *Annals of Physics* **311**, 431 (2004).
- [10] A. Kitagawa, M. Takeoka, M. Sasaki, and A. Chefles, *Phys. Rev. A* **73**, 042310 (2006).
- [11] T. Opatrný, G. Kurizki, and D.-G. Welsch, *Phys. Rev. A* **61**, 032302 (2000).
- [12] P. T. Cochrane, T. C. Ralph, and G. J. Milburn, *Phys. Rev. A* **65**, 062306 (2002).
- [13] S. Olivares, M. G. A. Paris, and R. Bonifacio, *Phys. Rev. A* **67**, 032314 (2003).
- [14] A. I. Lvovsky, H. Hansen, T. Aichele, O. Benson, J. Mlynek, and S. Schiller, *Phys. Rev. Lett.* **87**, 050402 (2001).
- [15] A. Zavatta, S. Viciani, and M. Bellini, *Phys. Rev. A* **70**, 053821 (2004).
- [16] A. Ourjountsev, R. Tualle-Brouiri, and P. Grangier, *Phys. Rev. Lett.* **96**, 213601 (2006).
- [17] S. A. Babichev, J. Appel, and A. I. Lvovsky, *Phys. Rev. Lett.* **92**, 193601 (2004).
- [18] M. D’Angelo, A. Zavatta, V. Parigi, and M. Bellini, *arXiv:quant-ph/0602150* (2006).
- [19] A. Ourjountsev, R. Tualle-Brouiri, J. Laurat, and P. Grangier, *Science* **312**, 83 (2006), published online 9 March 2006 (10.1126/science.1122858).
- [20] J. S. Neergaard-Nielsen, B. M. Nielsen, C. Hettich, K. Mølmer, and E. S. Polzik, *arXiv:quant-ph/0602198* (2006).
- [21] J. Wenger, A. Ourjountsev, R. Tualle-Brouiri, and P. Grangier, *Eur. Phys. J. D* **32**, 391 (2005).
- [22] G. Vidal and R. F. Werner, *Phys. Rev. A* **65**, 032314 (2002).
- [23] R. García-Patrón, J. Fiurášek, N. J. Cerf, J. Wenger, R. Tualle-Brouiri, and P. Grangier, *Phys. Rev. Lett.* **93**, 130409 (2004).
- [24] H. Nha and H. J. Carmichael, *Phys. Rev. Lett.* **93**, 020401 (2004).
- [25] J. Řeháček, Z. Hradil, and M. Ježek, *Phys. Rev. A* **63**, 040303(R) (2001).
- [26] A. I. Lvovsky, *J. Opt. B: Quantum Semiclass. Opt* **6**, S556 (2004).